forests

MDPI

Article

Effects of the Co-Application of Glucose, Nitrogen, and Elevated Temperature on Buried Black Soil Carbon in a Cool Temperate Deciduous Broad-Leaved Forest

Yasuo Iimura * and Daichi Tanaka

School of Environmental Science, The University of Shiga Prefecture, 2500 Hassakacho, Hikone 522-8533, Japan; os14dtanaka@ec.usp.ac.jp

* Correspondence: iimura.y@ses.usp.ac.jp

Abstract: Accurately predicting the feedback mechanisms between forest ecosystem carbon cycling and climate change is crucial for effective climate mitigation. Understanding soil organic carbon (SOC) responses to the combined impacts of plant biomass, litter, and nitrogen deposition, especially regarding temperature sensitivity, is essential but remains poorly understood. We conducted incubation experiments using buried black soil from a cool temperate deciduous broad-leaved forest in Japan, which has high C content and a highly stable molecular structure. The stepwise addition of glucose and a temperature increase from 15 to 35 °C accelerated SOC mineralization by 74.0 mg C kg^{-1} with a positive priming effect (PE) during the 49-day incubation period, while the simultaneous addition of nitrogen had no significant effect on this phenomenon, with SOC mineralization measured at 75.5 mg C kg^{-1}. Conversely, glucose mineralization was significantly accelerated by 10%, from 241.0 to 261.3 mg C kg^{-1}, by stepwise nitrogen addition and temperature increase. Under the combined impacts, the Q_{10} value of the soil increased significantly from 1.6 to 2.0 compared to that in the unmodified conditions, primarily due to the stepwise addition of glucose. We also found a strong positive correlation between activation energy (E_a) and Q_{10}. This result strongly supports the carbon quality–temperature (CQT) hypothesis. These results likely stem from interactions between SOC quality and carbon availability, suggesting that, in the future, climate change is likely to have a positive feedback effect, especially on buried black soils.

Keywords: black soil; forest; priming effect; $\delta^{13}C$; nitrogen deposition; temperature sensitivity

Citation: Iimura, Y.; Tanaka, D. Effects of the Co-Application of Glucose, Nitrogen, and Elevated Temperature on Buried Black Soil Carbon in a Cool Temperate Deciduous Broad-Leaved Forest. *Forests* **2024**, *15*, 1057. https://doi.org/10.3390/f15061057

Academic Editor: Zhangcai Qin

Received: 24 May 2024
Revised: 13 June 2024
Accepted: 17 June 2024
Published: 19 June 2024

1. Introduction

Soils represent the largest terrestrial carbon reservoir and are intricately linked to atmospheric CO_2, plant biomass, and microbial biomass through the carbon cycle [1]. The dynamics of soil organic carbon (SOC), particularly its decomposition and accumulation, are of significant concern because they are influenced by climate change and provide critical feedback [2]. Therefore, understanding SOC dynamics within the context of climate change is crucial for developing accurate global warming prediction models and formulating effective mitigation and adaptation strategies [3,4].

Many studies on the warming response of SOC in forest ecosystems have been reported based on both field and incubation experiments, often expressing it as Q_{10} (the proportional increase in CO_2 released by soil heterotrophic microbes for a 10 °C increase in temperature). While the Q_{10} values vary across different soils (ranging from approximately 2 to 5), the factors controlling Q_{10} are not fully understood due to the complexity of soil environments [5,6]. The carbon quality–temperature (CQT) hypothesis suggests that low-quality SOC, which requires a higher activation energy (E_a) for mineralization, exhibits a greater Q_{10} than high-quality SOC [2,7]. Recent molecular chemical structure analyses of SOC directly support this quality hypothesis [8]. Thus, it is becoming increasingly clear that the quality of SOC is a crucial factor in determining Q_{10}.

Global warming is expected to affect not only soils but also the above-ground vegetation. Increased atmospheric CO_2 levels are anticipated to enhance plant growth through photosynthesis in many ecosystems [9,10], likely increasing the influx of plant-derived biodegradable organic material—such as litter, dead roots, and root exudates—into the soil. These changes in SOM mineralization rates due to plant-derived components are known as the priming effect (PE) [11,12]. The PE varies with the soil conditions—temperature [13], moisture [14], and the quality and quantity of organic matter supplied [15,16]—and has shown positive [17–19], neutral [20], and negative [21–23] outcomes in different soils. Therefore, considering the PE based on plant–soil interactions is essential for accurately understanding the warming response of SOC.

Additionally, nitrogen deposition is emerging as a significant factor influencing future forest soil dynamics [24]. Projections by Galloway et al. (2004) [25] suggest a doubling of nitrogen deposition by 2050 relative to 1990, primarily in the form of inorganic compounds (NO_3-N, NH_4-N), raising concerns over its impact on forest SOC dynamics. Based on this prediction, it is highly likely that nitrogen deposition will exceed 10–25 kg-N ha^{-1} $year^{-1}$ in many forests, leading to significant nitrogen leaching. This, in turn, is a major concern because of its potentially significant impact on deep soils. Studies, including a meta-analysis by Janssens et al. (2010) [26], have shown that nitrogen deposition generally inhibits SOC degradation, underscoring the potential of nitrogen to suppress the microbial degradation of SOC. Recent studies also demonstrate similar trends [27,28], suggesting that nitrogen deposition in soils generally has a high potential to inhibit SOC mineralization. Several reports have also examined the effect of nitrogen deposition on the temperature sensitivity of soil. For example, it was reported that nitrogen deposition does not change or decreases Q_{10} in semi-arid soils [29], whereas nitrogen deposition increases Q_{10} by 1.4 times in subtropical soils [30]. This suggests that the effect of nitrogen deposition on Q_{10} varies considerably depending on the soil environment.

In recent years, studies on the dynamics of SOC related to the interaction between labile C supply and nitrogen deposition have also gradually increased. In a study on deep soils (60–70 cm) from subtropical forests in China, a leaf litter supply (*M. macclurei* and *P. massoniana*) promoted a positive PE, but nitrogen (NO_3-N, NH_4-N) addition reduced the intensity of this effect [16]. Similarly, in a cropping experiment with subtropical forest soils from China, it was reported that the cumulative PE associated with glucose addition was lower after long-term nitrogen addition compared to that obtained without nitrogen addition [19]. Thus, it was reported that the SOC response to the simultaneous addition of labile C and inorganic nitrogen reflects the interaction effects of the individual additions. Studies on the temperature sensitivity of SOC in response to the simultaneous addition of labile C and nitrogen deposition are extremely limited to date. For example, a study by Li et al. (2017) [31] using subtropical soils reported that the simultaneous addition of nitrogen suppressed the PE compared to the addition of glucose alone, and this phenomenon was more pronounced at 25 °C than at 15 °C. This suggests that the temperature sensitivity of SOC changes in response to labile C addition may be further altered by the concurrent addition of nitrogen. However, there are few studies on this topic, and more research is needed as there are many unknowns.

Volcanic ash soil is a major type of soil in Japan, characterized by very thick, dark-colored A horizons with a large amount of organo–mineral complexes of dark-colored organic matter associated with short-range order minerals (particularly allophane and imogolite) and/or monomeric Al and Fe ions (i.e., active Al and Fe) [32,33]. Although this dark-colored SOC is hypothesized to be very stable, the temperature sensitivity of SOC turnover and the PE in this Japanese black soil remain highly uncertain, especially in buried black layers [34,35].

To gain a deeper understanding of the warming response of forest SOC, it is crucial to consider not only the warming itself but also the combined effects of an increased supply of labile organic matter derived from plants and nitrogen deposition. As mentioned above, while there have been relatively many studies of the warming response of SOC to individual

factors such as labile C and nitrogen addition, very few studies have examined the warming response of soil under the combined effects of labile C and nitrogen deposition. In addition, none have focused on deep soils, which are key to the warming response of SOC. The aim of this study was to quantitatively assess the temperature sensitivity of SOC under these combined impacts. To achieve this objective, we conducted incubation experiments with stepwise temperature increases while simultaneously adding ^{13}C-labeled glucose and inorganic nitrogen.

2. Materials and Methods

2.1. Soil Sample

A soil sample was collected from the Takayama Experimental Forest, River Basin Research Center, Gifu University, Japan (36°08′ N, 137°25′ E, 1425 m above sea level). Detailed descriptions of this site are available in previous studies [35,36]. In summary, the mean annual temperature is 7.3 °C, and the mean annual precipitation is approximately 2400 mm (2014–2015). Snow covers the ground from December to April, with depths typically ranging from 1 to 2 m. The dominant tree species include *Quercus crispula* and *Betula platyphylla* var. *japonica*. The forest floor is densely covered by dwarf bamboo (*Sasa senanensis*). The soil at this site is classified as Andisol (Soil Survey Staff, 2014). We collected the soil sample from the deepest 40–50 cm layer of the buried A horizon within a 1 m soil profile. After collection, the fresh soil sample was sieved through a 2 mm mesh, and all visible plant debris and roots were meticulously removed using tweezers. The fresh soil sample was then stored in a refrigerator at 5 °C for approximately 10 days prior to being used in the incubation experiment. Subsamples for soil characterization were air-dried and processed in the same manner as described above. Table 1 presents several soil characteristics from this study, as reported by Iimura et al. (2020) [35].

Table 1. Characteristics of the soil used in this study as demonstrated by Iimura et al. (2020) [35].

Depth	pH			T-C	C:N Ratio	MI [1]	δ^{13}C	^{14}C Age [2]
(cm)	(H_2O)	(KCl)	(NaF)	(g kg^{-1})			(‰)	(YrBP)
40–50	5.1	4.3	11.5	89.4	16.0	1.64	−19.8	4764–5082

[1] The melanic index of soil humus. [2] The ^{14}C age of soil samples from 40 to 45 cm and from 45 to 50 cm, respectively.

2.2. Incubation Experiment

The experimental units comprised fresh sieved soil (equivalent to 50 g of oven-dried samples) placed in 500 mL jars and were incubated at progressively increasing temperatures of 15, 25, and 35 °C over a 49-day period. This incubation continued until CO_2 emission from the soil stabilized at each temperature condition (7 days at 15 °C, 21 days at 25 °C, and 21 days at 35 °C). Following a 3-day preincubation at 15 °C, the incubation commenced. Glucose (2.188 atom%) was added to the soil at a rate of 0.25 g of C-glucose per kg of dry soil, associated with temperature increases from 15 °C to 25 °C and from 25 °C to 35 °C, resulting in a total of 0.5 g of C-glucose per kg of dry soil. This was based on the amount of root exudate in temperate forests [20]. Additionally, mineral nitrogen ($(NH_4)_2SO_4$) was applied at a rate of 50 mg of NH_4^+-N kg^{-1}, timed to coincide with carbon addition, based on the projected future deposition rates of mineral nitrogen (NH_4^+ and NO_3^-) in terrestrial ecosystems [25]. Soil samples without glucose and mineral nitrogen served as controls and were similarly mixed to maintain a consistent physical disturbance. The incubation experiment consisted of four treatments (each with three replicates): soil only (S), soil with mineral nitrogen (SN), soil with glucose (SC), and soil with glucose plus mineral nitrogen (SCN). The soil moisture content was adjusted to 60% of the water-holding capacity using distilled water throughout the incubation period. CO_2 emissions were captured in a NaOH solution at 7, 14, 21, 28, 35, 42, and 49 days of incubation. A glass vial containing 20 mL of 0.2 M NaOH solution was placed in each jar to trap the emitted CO_2, and the jars were sealed after being flushed with CO_2-free air. Each time the NaOH solution

was replaced, the jars were again flushed with CO_2-free air. The carbon content of the NaOH solution was determined by titration [16]. The $\delta^{13}C$ of CO_2 was analyzed using an EA/IRMS continuous-flow system following carbonate precipitation with excess $BaCl_2$ and filtration [35] every 7 days during the incubation. $\delta^{13}C$ measurements were repeated until the standard deviation was less than 0.2‰. Following incubation, the soil was immediately freeze-dried and stored for subsequent microbial biomass analysis.

2.3. Calculation of PE and Q_{10} and E_a Values

The substrate (glucose) added to the soil allowed for the separation of the respiration rates (mg CO_2-C kg^{-1} soil) of the native soil C (R_{soil}) and of the substrate (R_{sub}) using mass balance equations [35,37] as follows:

$$R_{soil} + R_{sub} = R_{total}$$

$$R_{soil} \times \delta^{13}C_{soil} + R_{sub} \times \delta^{13}C_{sub} = R_{total} \times \delta^{13}C_{total}$$

where $\delta^{13}C_{soil}$ is $\delta^{13}C$ of the soil C, $\delta^{13}C_{sub}$ is $\delta^{13}C$ of glucose C, R_{total} is the total CO_2 emitted by the soil with glucose, and $\delta^{13}C_{total}$ is its $\delta^{13}C$.

The PE (mg C-CO_2 kg^{-1} soil) induced by the addition of the substrate was calculated as:

$$PE = (R_{soil} \text{ soil with substrates}) - (R_{soil} \text{ control soil})$$

where (R_{soil} control soil) is the CO_2 emitted by the control soil.

The cumulative CO_2 released under each temperature condition was converted to the daily emission rate to calculate the Q_{10} value for the range of 15–35 °C. This calculation was performed separately for total CO_2 and soil-derived CO_2. According to Yashiro et al. (2011) [38], the temperature dependence of CO_2 efflux and Q_{10} is calculated as:

$$R = R_0 \exp(kT)$$

$$Q_{10} = \exp^{10k}$$

where R is the respiration rate, R_0 and k are fitting parameters, and T is temperature.

The activation energy (E_a) was determined using the Arrhenius equation [39]. Following the procedures outlined by He et al. (2024) [7], the following calculation was perfromed:

$$k = A\exp^{(-Ea/RT)}$$

Here, k denotes the SOM mineralization rate at temperature T (in Kelvin), A is the pre-exponential factor, E_a represents the activation energy required (in Joules per mole), and R is the universal gas constant (8.314 J mol^{-1} K^{-1}) [2]. By applying the natural logarithm to both sides of the equation, E_a was determined as the slope of the linear relationship between $-1/RT$ and the natural logarithm of k.

2.4. Microbial Biomass Carbon

Microbial biomass C in each soil sample after the incubation period (49 days) was determined using the adenosine triphosphate (ATP) method [40]. Soil ATP was sequentially extracted with DMSO and Na_3PO_4. First, 10 mL of DMSO was added to 1 g of soil (freeze-dried), and the mixture was extracted on a stirrer for 2 min. Subsequently, 40 mL of a 0.01 M Na_3PO_4 solution was added to the same soil, and the mixture was extracted on a stirrer for 2 min, followed by sonication for 2 min. Then, 1 mL of the supernatant was immediately added to 10 mL of a 0.01 M glycine solution (containing 0.005 M Mg-EDTA), mixed, and then used for ATP measurement. ATP was analyzed using a luminometer and a test kit (Lumitester PD-30 and LuciPac PEN, Kikkoman Biochemifa Company, Tokyo, Japan).

The $\delta^{13}C$ values of microbial biomass were measured according to Fontaine et al. (2004) [41]. Each 5 g aliquot of soil after incubation was exposed to ethanol-free chloroform for 2 days and then shaken for 1 h with 20 mL of 30 mM K_2SO_4. The K_2SO_4 extracts were filtered

through 0.3 µm glass fiber filters. The K_2SO_4 extracts were then lyophilized, and the recovered crystals were stored in a glass desiccator until the analysis of $\delta^{13}C$.

The contribution ratios of labelled microbial biomass (MB_{sub}) and unlabelled microbial biomass (MB_{soil}) to total microbial biomass C (MB_{total}) were estimated using mass balance equations [41] as follows:

$$MB_{soil} + MB_{sub} = MB_{total}$$

$$MB_{soil} \times \delta^{13}C_{soil} + MB_{sub} \times \delta^{13}C_{sub} = MB_{total} \times \delta^{13}C_{mic}$$

where $\delta^{13}C_{soil}$ is $\delta^{13}C$ of the soil C, $\delta^{13}C_{sub}$ is $\delta^{13}C$ of glucose C, and $\delta^{13}C_{mic}$ is $\delta^{13}C$ of each K_2SO_4 extracts.

2.5. Statistical Analysis

For total CO_2 emission, soil-derived CO_2 emission, and microbial biomass carbon, one-way analysis of variance (ANOVA) was performed. A *t*-test was performed to compare glucose-derived CO_2 emission from SC and SCN and primed CO_2 for each treatment and the control. All statistical analyses were performed using StatPlus:mac Pro (version 7.8.11).

3. Results

3.1. CO_2 Emission

3.1.1. Total CO_2

Figure 1 shows the temporal changes in total CO_2 emissions during the incubation period. The differences in total CO_2 emissions between treatments tended to increase over time. Notably, significant increases were observed in the SC and SCN samples, where glucose was added, particularly on day 14 of incubation when the temperature increased from 15 °C to 25 °C and after day 28 when the temperature increased from 25 °C to 35 °C. At the end of the 25 °C incubation, CO_2 emissions from SC and SCN were 3.7 times higher than from S. At the end of the 35 °C incubation, CO_2 emissions were 3.8 times higher from SC and 4.0 times higher from SCN compared to the S, respectively. However, SN did not show such trends and behaved similarly to S.

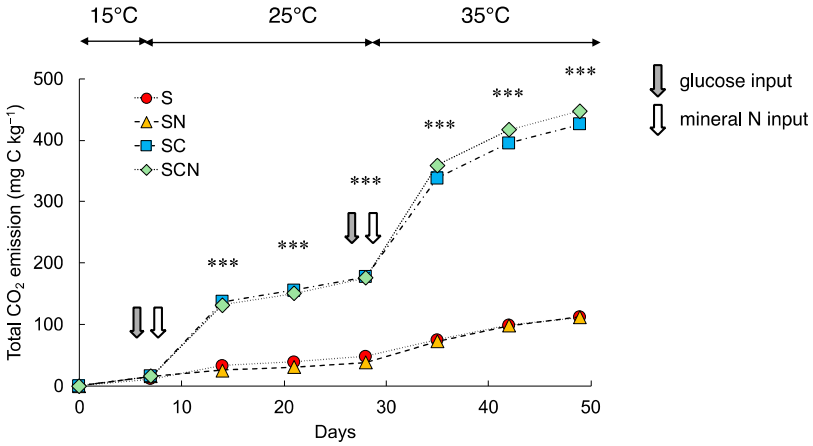

Figure 1. Cumulative total CO_2 emissions from each treatment. S: soil only (control); SN: soil with mineral N; SC: soil with glucose; SCN: soil with glucose plus mineral N. Bars indicate the standard error of the mean (n = 3). Asterisks (***) indicate significant differences at $p < 0.005$ by one-way analysis of variance (ANOVA).

3.1.2. Glucose and Soil-Derived CO_2

Figure 2a,b show the temporal changes in CO_2 emissions from soil and glucose during the incubation period, respectively. The temporal changes in CO_2 emissions from the soil showed a trend similar to that of the changes in total CO_2 emissions, shown in Figure 1, with significantly higher values for SC and SCN where glucose was added. SC and SCN exhibited significant changes on days 14 and 28, when glucose was added and the

temperature increased, with CO_2 emissions being 1.7 times higher than from S at the end of the 25 °C incubation and 1.7 times higher at the end of the 35 °C incubation. In contrast, S and SN showed similar trends with no significant differences between them. The CO_2 emissions from glucose were generally higher than those from soil, with 1.3 times higher emissions from SC and 1.4 times higher from SCN. Up to day 28 at 25 °C, there were no significant differences between SC and SCN, but significantly higher values were observed for the SC treatment after day 28 when the temperature increased to 35 °C. This trend continued until the end of the incubation period.

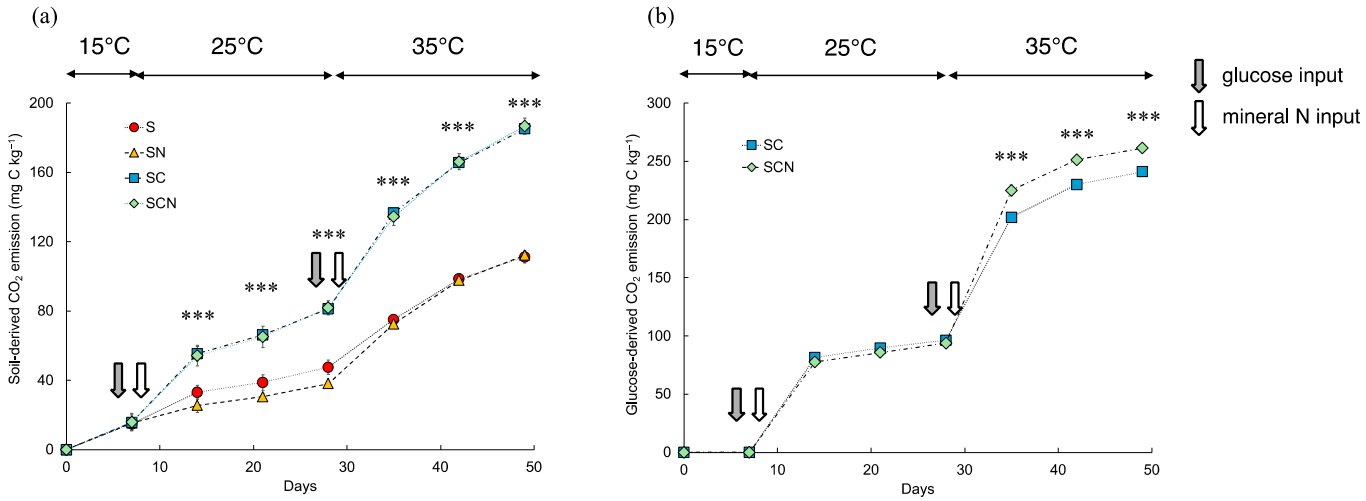

Figure 2. (**a**) Cumulative soil-derived CO_2 and (**b**) glucose-derived CO_2 emissions from each treatment. S: soil only (control); SN: soil with mineral N; SC: soil with glucose; SCN: soil with glucose plus mineral N. Bars indicate the standard error of the mean (n = 3). Asterisks (***) indicate significant differences at $p < 0.005$ by one-way analysis of variance (ANOVA).

3.2. Priming Effect

Table 2 shows the calculated PE from soil-derived CO_2 emissions in each treatment. SN showed a trend of lower CO_2 emissions compared to S throughout the incubation period, ranging from −9.5 to 1.0 mg C kg^{-1}, but this difference was not significant, and the PE remained neutral. In contrast, SC and SCN had significantly higher soil-derived CO_2 emissions compared to S, except at 15 °C, with PE values at 25 °C and 35 °C ranging from 22.4 to 74.0 mg C kg^{-1} and from 21.1 to 75.5 mg C kg^{-1}, respectively. The PE tended to increase at higher temperatures and with longer incubation periods.

Table 2. Primed CO_2 emissions from each treatment. SN: soil with mineral N; SC: soil with glucose; SCN: soil with glucose plus mineral N. Asterisks (*, **, ***) indicate significant differences at $p < 0.05$, $p < 0.01$, and $p < 0.005$, respectively (t-test).

Days	Temp. °C	Primed CO_2 (mg C kg^{-1})		
		SN	SC	SCN
7	15	0.6 ± 1.9	0.8 ± 2.9	1.1 ± 3.3
14	25	−7.4 ± 2.9	22.4 ± 2.9 *	21.1 ± 3.6 *
21	25	−8.3 ± 2.4	27.3 ± 2.6 **	26.3 ± 3.8 *
28	25	−9.5 ± 2.2	33.7 ± 2.2 ***	34.3 ± 2.9 ***
35	35	−2.6 ± 1.3	61.5 ± 0.4 ***	59.2 ± 2.6 ***
42	35	−0.8 ± 1.8	67.0 ± 1.4 ***	67.6 ± 2.7 ***
49	35	1.0 ± 2.1	74.0 ± 1.7 ***	75.5 ± 2.9 ***

3.3. Temperature Sensitivity

3.3.1. Q_{10} Values

The results for Q_{10} calculated from total CO_2 emissions and soil-derived CO_2 emissions are shown in Figure 3a,b. Both Q_{10} values exhibited similar trends across different treatment intervals, with significantly higher values for SC and SCN compared to S and SN. The Q_{10} for total CO_2 emissions ranged from 1.6 to 3.3, with the lowest value in S, and the highest value in SCN. Additionally, the Q_{10} of soil-derived CO_2 emissions ranged from 1.6 to 2.0, with the lowest value in S, and higher values in both SC and SCN.

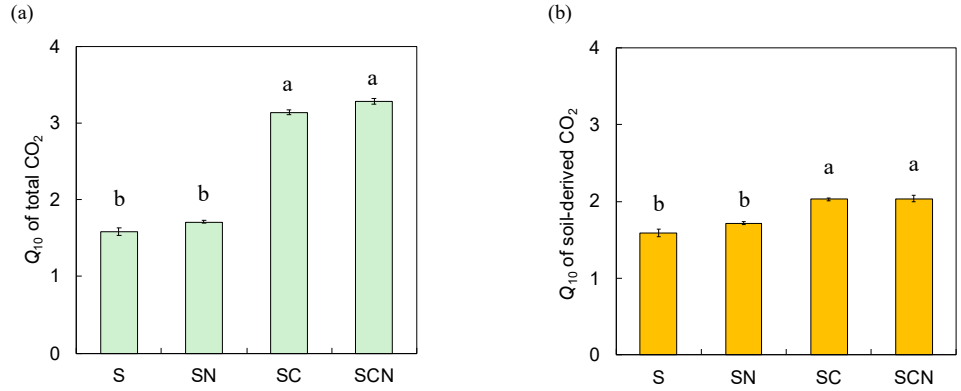

Figure 3. Q_{10} values of (**a**) total and (**b**) soil-derived CO_2 emissions from each treatment. S: soil only (control); SN: soil with mineral N; SC: soil with glucose; SCN: soil with glucose plus mineral N. Bars indicate the standard error of the mean (n = 3). Values with different letters are significantly different ($p < 0.05$) by Tukey's HSD post hoc test.

3.3.2. Activation Energy (E_a)

The activation energy (E_a) for each treatment plot showed a similar trend to that of Q_{10} (Figure 4a,b). For total CO_2 emissions, E_a ranged from 34 to 88 kJ mol^{-1}, with significantly higher values for SC and SCN compared to S and SN. For soil-derived CO_2 emissions, E_a ranged from 34 to 53 kJ mol^{-1}, and similar to what observed for total CO_2 emissions, the SC and SCN samples showed significantly higher values compared to S and SN. A very strong positive correlation (r = 0.999, $p < 0.001$) was observed between Q_{10} and E_a for both total CO_2 and soil-derived CO_2 (Figure 5a,b).

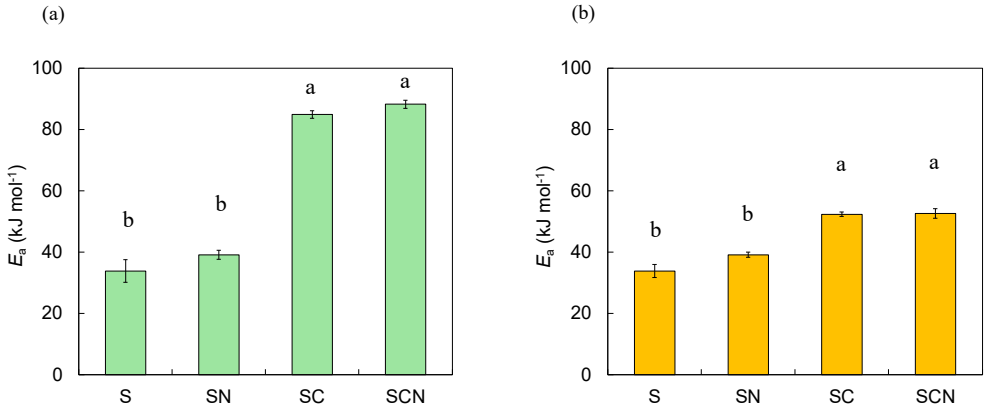

Figure 4. Activation energy (E_a) calculated from (**a**) total CO_2 and (**b**) soil-derived CO_2 for each treatment. S: soil only (control); SN: soil with mineral N; SC: soil with glucose; SCN: soil with glucose plus mineral N. Bars indicate the standard error of the mean (n = 3). Values with different letters are significantly different ($p < 0.05$) by Tukey's HSD post hoc test.

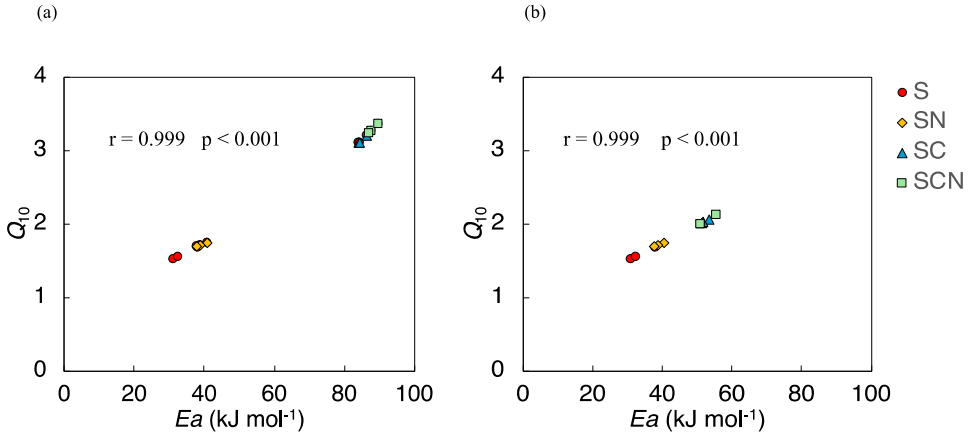

Figure 5. Relationship between Q_{10} and E_a in (**a**) total CO_2 and (**b**) soil-derived CO_2 for each treatment. S: soil only (control); SN: soil with mineral N; SC: soil with glucose; SCN: soil with glucose plus mineral N.

3.4. Microbial Biomass Carbon

Figure 6 shows the results of microbial biomass for each treatment plot at the end of the incubation period. The microbial biomass in each treatment plot ranged from 45 to 85 mg C kg^{-1}. The differences among the treatment plots showed a similar trend to that of Q_{10} and activation energy, with significantly higher values for the SC and SCN plots compared to the S and SN plots. Additionally, in the SC and SCN plots, 96% of the total biomass was unlabeled.

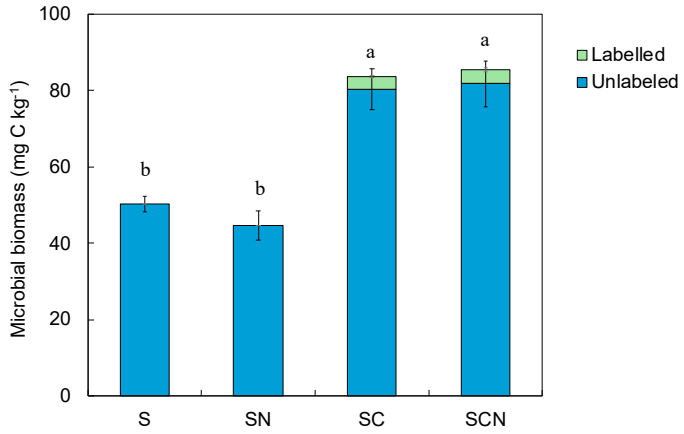

Figure 6. ^{13}C-labeled (green) and unlabeled (blue) microbial biomass in each treatment plot. S: soil only (control); SN: soil with mineral N; SC: soil with glucose; SCN: soil with glucose plus mineral N. Bars indicate the standard error of the mean (n = 3). Values with different letters are significantly different ($p < 0.05$) by Tukey's HSD post hoc test.

4. Discussion

In this study, the addition of glucose to buried black SOC resulted in the accelerated decomposition of SOC due to a positive PE. Additionally, this trend intensified with an increasing temperature from 15 °C to 35 °C. The concurrent nitrogen addition enhanced the mineralization and the temperature sensitivity of the added glucose, while having a minimal impact on the mineralization of SOC. This suggests that future increases in nitrogen deposition due to climate change may not be a significant factor in the mineralization of buried black SOC. On the other hand, the addition of nitrogen to soil may promote the mineralization and assimilation of glucose through microbial activity and further stabilize it onto soil particles, effects which could be further accelerated by rising temperatures. Hereafter, we will discuss the effects of the coexistence of glucose addition, nitrogen

addition, and warming on the dynamics and temperature sensitivity of glucose and buried black SOC.

4.1. Glucose Dynamics

Throughout the 49-day incubation period, glucose was added to the soil in two stages, i.e., at a temperature from 15 °C to 25 °C and at a temperature from 25 °C to 35 °C, each time adding 0.25 g C kg^{-1}, resulting in a total of 0.5 g C kg^{-1}. The CO_2 derived from glucose, calculated using stable isotope ratios, amounted to approximately 0.25 g C kg^{-1}, which is half of the total added amount. In contrast, the carbon derived from glucose detected in the soil microbial biomass at the end of the incubation was only about 3 to 4 mg C kg^{-1} (Figure 6). Considering that glucose is not adsorbed onto soil particles [42], is a major substrate assimilated by soil microorganisms [43], and is available to most microorganisms [44], it is possible that approximately half of the added glucose was assimilated by microorganisms and that its residues were stabilized in the soil [45]. Such soil carbon sequestration processes mediated by microbial assimilation have recently attracted attention [46,47]. Additionally, the temperature sensitivity of glucose was significantly higher in SCN than in SC (Figure 2b), suggesting that the mineralization, assimilation, and stabilization of glucose in soil are enhanced by nitrogen addition. These phenomena have been described by the stoichiometric theory, which indicates that the mineralization of labile organic matter dominated by r-strategists is particularly accelerated by the addition of nitrogen [48]. Thus, it is possible that glucose, through interactions with black SOC mediated by microorganisms, was converted into a relatively stable part of SOC. This might be one of the reasons why the Q_{10} of SOC was significantly higher in SC and SCN (see Section 4.3). Directly elucidating these processes remains a challenge for future research.

4.2. SOC Dynamics

The mineralization rate of SOC exhibited a general increasing trend, particularly with the addition of glucose, which showed a positive PE that accelerated by rising temperatures (Figure 2, Table 1). In contrast, no significant effect of nitrogen addition was observed. Research on the PE induced by the addition of labile organic matter (carbon and nitrogen) and its temperature sensitivity has intensified in recent years due to their importance. For instance, a 57-day incubation experiment with temperate forest soil in China demonstrated a negative PE at 5 °C following glucose addition, while positive PEs were observed at 15 °C and 25 °C, with the magnitude increasing with temperature [14]. Additionally, an incubation study using temperate grassland soil collected from a long-term, 7-year field warming experiment showed that the addition of wheat straw accelerated SOM mineralization by 12.7%, indicating that warming enhances SOM mineralization via PE [49]. These findings support our results. Conversely, Li et al. (2023) [50] conducted a meta-analysis of 146 observations from 57 independent soils worldwide, showing that experimental warming significantly suppressed ΔPE (the difference in PE between control and warming treatments) by 0.26. Such contrasting results highlight the complex effects of warming on the PE. The PE and its response to warming in soil are likely dependent on the quantity and quality of the added substrate, particularly the nitrogen content relative to that of labile carbon. SOM is generally more recalcitrant than newly added labile organic matter, and it is well known that the PE is promoted in a positive direction by nitrogen deficiency (high CN ratio) relative to labile carbon content [41,48]. This phenomenon is widely recognized as the N mining theory, a key PE mechanism that also significantly influences the temperature dependence of the PE [37,41,48]. The aforementioned meta-analysis also found that agricultural soils, which are less prone to nitrogen limitation, exhibited a high suppression rate of 0.43, whereas the PE in nitrogen-limited forest soils remained unaffected by warming [50]. Our findings suggest that the positive PE of SOC accelerated with rising temperatures regardless of nitrogen addition, indicating a potential absolute nitrogen limit for SOM mineralization. Conversely, the mineralization of glucose was accelerated by nitrogen addition in this study, suggesting that the optimal CN ratio for substrate utilization may

vary. A detailed evaluation of the relationship between the CN ratio of more labile forms and the decomposition characteristics of substrates with different recalcitrance levels could provide clearer insights.

4.3. Temperature Sensitivity

In comparison to the S and SN treatments without glucose addition, the SC and SCN treatments with incremental glucose additions showed significantly higher Q_{10} values for both total CO_2 and SOC-derived CO_2 (Figure 3a,b). Although the main factors influencing the Q_{10} of SOC remain uncertain, the soil carbon energy state [51] and SOC quality [2] are often recognized as key factors. Recently, Zhang et al. (2024) [52] demonstrated that the interaction between SOC quality and carbon availability universally impacts Q_{10}. Specifically, when carbon availability is not limited, SOC quality determines the sensitivity, with more recalcitrant SOC exhibiting a higher Q_{10}. Conversely, when carbon availability is limited, substrate availability determines Q_{10}. The black SOC used in this study is known to be of very low quality with high aromaticity compared to other SOM types [29,32], suggesting that increased carbon availability due to glucose addition in SC and SCN resulted in higher Q_{10} values compared to those for S and SN. This is further supported by the strong positive correlation between E_a and Q_{10} (Figure 5b). The CQT hypothesis, widely known [2,7], posits that lower quality SOC requires higher E_a. Additionally, Wagai et al. (2013) [8] analyzed the relationship between the SOC quality of the light fraction (<1.6 g cm^{-3}) and temperature sensitivity using volcanic ash soil, finding that higher proportions of carbon resistant to enzymatic decomposition (aromatic carbon and aliphatic carbon) were associated with higher Q_{10} values. Considering these findings along with the theory of SOC quality–carbon availability interactions, it can be inferred that low-quality SOC, with high proportions of aromatic and aliphatic carbon, exhibits increased Q_{10} in response to the supply of highly available glucose.

5. Conclusions

To elucidate the response of SOC to the combined impacts of glucose addition, nitrogen addition, and warming, particularly its temperature sensitivity (Q_{10}, E_a), we conducted an incubation experiment using buried black soil as the test soil. The results revealed the following:

1. The stepwise addition of glucose significantly increased the Q_{10} of SOC, whereas the simultaneous addition of nitrogen had no effect on Q_{10}.

2. The decomposition of glucose increased with the stepwise addition of nitrogen, especially under high-temperature conditions (35 °C), with approximately half of the glucose being released as CO_2, and the remainder retained in the soil.

3. There was a strong positive correlation between E_a and Q_{10}, strongly supporting the CQT hypothesis.

Furthermore, the findings in points 1 and 3 are likely the result of the interaction between SOC quality and carbon availability, and point 2 suggests that a portion of the added glucose was stabilized in the soil through microbial activity. The results of this study provide important insights for more accurately predicting the dynamics of highly stable buried black SOC.

Author Contributions: Conceptualization, Y.I.; validation, Y.I. and D.T.; formal analysis, Y.I. and D.T.; investigation, Y.I. and D.T.; data curation, Y.I.; writing—original draft preparation, Y.I.; writing—review and editing, Y.I. and D.T.; project administration, Y.I.; funding acquisition, Y.I. All authors have read and agreed to the published version of the manuscript.

Funding: This research was supported by the Japan Society for the Promotion of Science KAKENHI (17K00524, 20K12138) to Y.I.

Data Availability Statement: No new data were created or analyzed in this study. Data sharing is not applicable to this article.

Acknowledgments: We thank the members of the Laboratory of Soil Science at The University of Shiga Prefecture for their discussion on this research.

Conflicts of Interest: The authors declare no conflicts of interest.

References

1. Lal, R. Managing Soils and Ecosystems for Mitigating Anthropogenic Carbon Emissions and Advancing Global Food Security. *BioScience* **2010**, *60*, 708–721. [CrossRef]
2. Davidson, E.A.; Janssens, I.A. Temperature Sensitivity of Soil Carbon Decomposition and Feedbacks to Climate Change. *Nature* **2006**, *440*, 165–173. [CrossRef]
3. Amelung, W.; Bossio, D.; Vries, W.; Kögel-Knabner, I.; Lehman, J.; Amundson, R.; Bol, R.; Collins, C.; Lal, R.; Leifeld, J.; et al. Towards a Global-Scale Soil Climate Mitigation Strategy. *Nat. Commun.* **2020**, *11*, 5427. [CrossRef]
4. Lal, R. Managing Soil Carbon Sequestration to Mitigate Climate Change. *Geoderma* **2004**, *123*, 1–22. [CrossRef]
5. Conant, R.T.; Ryan, M.G.; Ågren, G.I.; Birge, H.E.; Davidson, E.A.; Eliasson, P.E.; Evans, S.E.; Frey, S.D.; Giardina, C.P.; Hopkins, F.M.; et al. Temperature and Soil Organic Matter Decomposition Rates—Synthesis of Current Knowledge and a Way Forward. *Glob. Biol.* **2011**, *17*, 3392–3404. [CrossRef]
6. Kirschbaum, M.U.F. The Temperature Dependence of Organic−Matter Decomposition−Still a Topic of Debate. *Soil Biol. Biochem.* **2011**, *38*, 2510–2518. [CrossRef]
7. He, P.; Li, L.J.; Dai, S.S.; Guo, X.L.; Nie, M.; Yang, X. Straw Addition and Low Soil Moisture Decreased Temperature Sensitivity and Activation Energy of Soil Organic Matter. *Geoderma* **2024**, *442*, 116802. [CrossRef]
8. Wagai, R.; Kishimoto-Mo, A.W.; Yonemura, S.; Shirato, Y.; Hiradate, S.; Yagawaki, Y. Linking Temperature Sensitivity of Soil Organic Matter Decomposition to its Molecular Structure, Accessibility, and Microbial Physiology. *Glob. Biol.* **2013**, *19*, 13–25. [CrossRef]
9. De Graaff, M.A.; van Groenigen, K.J.; Six, J.; Hungate, B.; van Kessel, C. Interactions Between Plant Growth and Soil Nutrient Cycling Under Elevated CO_2: A Meta-Analysis. *Glob. Biol.* **2006**, *12*, 2077–2091. [CrossRef]
10. Leppälammi-Kujansuu, J.; Salemaa, M.; Kleja, D.B.; Linder, S.; Helmisaari, H.S. Fine Root Turnover and Litter Production of Norway Spruce in a Long-Term Temperature and Nutrient Manipulation Experiment. *Plant Soil* **2014**, *374*, 73–88. [CrossRef]
11. Kuzyakov, Y.; Friedel, J.K.; Stahr, K. Review of Mechanisms and Quantification of Priming Effects. *Geoderma* **2000**, *32*, 1485–1498. [CrossRef]
12. Fontaine, S.; Mariotti, A.; Abbadie, L. The Priming Effect of Organic Matter: A Question of Microbial Competition? *Soil Biol. Biochem.* **2003**, *35*, 837–843. [CrossRef]
13. Ghee, C.; Neilson, R.; Hallett, P.D.; Robinson, D.; Paterson, E. Priming of Soil Organic Matter Mineralisation is Intrinsically Insensitive to Temperature. *Soil Biol. Biochem.* **2013**, *66*, 20–28. [CrossRef]
14. Feng, C.; Sun, H.; Zhang, Y. The Magnitude and Direction of Priming were Driven by Soil Moisture and Temperature in a Temperate Forest Soil of China. *Pedobiologia* **2021**, *89*, 150769. [CrossRef]
15. Blagodatskaya, E.; Kuzyakov, Y. Mechanisms of Real and Apparent Priming Effects and their Dependence on Soil Microbial Biomass and Community Structure: Critical Review. *Biol. Fertil. Soils* **2008**, *45*, 115–131. [CrossRef]
16. Wang, Q.; Wang, Y.; Wang, S.; He, T.; Liu, L. Fresh Carbon and Nitrogen Inputs Alter Organic Carbon Mineralization and Microbial Community in Forest Deep Soil Layers. *Soil Biol. Biochem.* **2014**, *72*, 145–151. [CrossRef]
17. Hamer, U.; Marschner, B. Priming Effects in Different Soil Types Induced by Fructose, Alanine, Oxalic Acid and Catechol Additions. *Soil Biol. Biochem.* **2005**, *37*, 445–454. [CrossRef]
18. Wang, Q.K.; Chen, L.C.; Yang, Q.P.; Sun, T.; Li, C.M. Different Effects of Single Versus Repeated Additions of Glucose on the Soil Organic Carbon Turnover in a Temperate Forest Receiving Long-Term N Addition. *Geoderma* **2019**, *341*, 59–67. [CrossRef]
19. Xu, M.; Zeng, Q.; Liu, Y.; Liu, C.; Zhang, Q.; Mei, K.; Yuan, X.; Zhang, X.; Chen, Y. Keystone Soil Microbial Modules Associated with Priming Effect under Nitrogen- and Glucose-Addition Treatments. *Forests* **2023**, *14*, 1207. [CrossRef]
20. Nottingham, A.T.; Griffiths, H.; Chamberlain, P.M.; Stott, A.W.; Tanner, E.V.J. Soil Priming by Sugar and Leaf-Litter Substrates: A Link to Microbial Groups. *Appl. Soil Ecol.* **2009**, *42*, 183–190. [CrossRef]
21. Qiao, N.; Schaefer, D.; Blagodatskaya, E.; Zou, X.; Xu, X.; Kuzyakoy, Y. Labile Carbon Retention Compensates for CO_2 Released by Priming in Forest Soils. *Glob. Change Biol.* **2014**, *20*, 1943–1954. [CrossRef]
22. Pegoraro, E.; Mauritz, M.; Bracho, R.; Ebert, C.; Dijkstra, P.; Hungate, B.A.; Konstantinidis, K.T.; Luo, Y.; Schädel, C.; Tiedje, J.M. Glucose Addition Increases the Magnitude and Decreases the Age of Soil Respired Carbon in a Long-Term Permafrost Incubation Study. *Soil Biol. Biochem.* **2018**, *129*, 201–211. [CrossRef]
23. Guenet, B.; Leloup, J.; Raynaud, X.; Bardoux, G.; Abbadie, L. Negative Priming Effect on Mineralization in a Soil Free of Vegetation for 80 Years. *Eur. J. Soil Sci.* **2010**, *61*, 384–391. [CrossRef]
24. Magnani, F.; Mencuccini, M.; Borghetti, M.; Berbigier, P.; Berninger, F.; Delzon, S.; Grelle, A.; Hari, P.; Jarvis, P.G.; Kolari, P.; et al. The Human Footprint in the Carbon Cycle of Temperate and Boreal Forests. *Nature* **2007**, *447*, 848–850. [CrossRef]

25. Galloway, J.N.; Dentener, F.J.; Capone, D.G.; Boyer, E.W.; Howarth, R.W.; Seitzinger, S.P.; Asner, G.P.; Cleveland, C.C.; Green, P.A.; Holland, E.A.; et al. Nitrogen Cycles: Past, Present, and Future. *Biogeochemistry* **2004**, *70*, 153–226. [CrossRef]
26. Janssens, I.A.; Dieleman, W.; Luyssaert, S.; Subke, J.A.; Reichstein, M.; Ceulemans, R.; Ciais, P.; Dolman, A.J.; Grace, J.; Matteucci, G.; et al. Reduction of Forest Soil Respiration in Response to Nitrogen Deposition. *Nat. Geosci.* **2010**, *3*, 315–322. [CrossRef]
27. Zhou, S.; Xiang, Y.; Tie, L.; Han, B.; Huang, C. Simulated Nitrogen Deposition Significantly Reduces Soil Respiration in an Evergreen Broadleaf Forest in Western China. *PLoS ONE* **2018**, *13*, e0204661. [CrossRef]
28. Chen, C.; Chen, H.Y. Mapping Global Nitrogen Deposition Impacts on Soil respiration. *Sci. Total Environ.* **2023**, *871*, 161986. [CrossRef]
29. Zang, C.; Niu, D.; Niu, D.; Hall, J.S.; Wen, H.; Li, X.; Fu, H.; Wan, C.; Elser, J.J. Effects of Simulated Nitrogen Deposition on Soil Respiration Components and Their Temperature Sensitivities in a Semiarid Grassland. *Soil Biol. Biochem.* **2014**, *75*, 113–123. [CrossRef]
30. Guo, Z.; Qiang, W.; He, J.; Han, X.; Tan, X.; Ludwig, B.; Shen, W.; Kuzyakov, Y.; Gunina, A. Nitrogen Deposition Raises Temperature Sensitivity of Soil Organic matter decomposition in subtropical forest. *Sci. Total Environ.* **2024**, *907*, 167925. [CrossRef]
31. Li, Q.; Tian, Y.; Zhang, X.; Xu, X.; Wang, H.; Kuzyakov, Y. Labile Carbon and Nitrogen Additions Affect Soil Organic Matter Decomposition More Strongly than Temperature. *Appl. Soil Ecol.* **2017**, *114*, 152–160. [CrossRef]
32. Iimura, Y.; Fujimoto, M.; Tamura, K.; Higashi, T.; Kondo, M.; Uchida, M.; Yonebayashi, K.; Fujitake, N. Black Humic Acid Dynamics During Natural Reforestation of Japanese Pampas Grass (*Miscanthus sinensis*). *Geoderma* **2013**, *57*, 60–67. [CrossRef]
33. Asano, M.; Wagai, R. Evidence of Aggregate Hierarchy at Micro- to Submicron Scales in an Allophanic Andisol. *Geoderma* **2014**, *216*, 62–74. [CrossRef]
34. Iimura, Y.; Tabara, I.; Izumitsu, K.; Fujitake, N. Priming Effect of the Addition of Maize to a Japanese Volcanic Ash Soil and its Temperature Sensitivity: A Short-Term Incubation Study. *Soil Sci. Plant Nutr.* **2019**, *65*, 444–450. [CrossRef]
35. Iimura, Y.; Tanaka, D.; Nagao, S.; Fujitake, N.; Ohtsuka, T. The Mineralization Rate of Black Soil Carbon in the Deep Layers of Japanese Volcanic Ash Soil may be Easily Accelerated by Labile Carbon Supply. *Soil Sci. Plant Nutr.* **2020**, *66*, 415–420. [CrossRef]
36. Cao, R.; Chen, S.; Yoshitake, Y.; Ohnishi, T.; Iimura, Y.; Ohtsuka, T. The Nitrogen Cycle of a Cool-Temperate Deciduous Broad-Leaved Forest. *Forests* **2024**, *15*, 725. [CrossRef]
37. Fontaine, S.; Henault, C.; Aamor, A.; Bdioui, N.; Bloor, J.M.G.; Maire, V.; Mary, B.; Revaillot, S.; Maron, P.A. Fungi Mediate Long Term Sequestration of Carbon and Nitrogen in Soil through their Priming Effect. *Soil Biol. Biochem.* **2011**, *43*, 86–96. [CrossRef]
38. Yashiro, Y.; Shizu, Y.; Adachi, T.; Ohtsuka, T.; Lee, N.Y.; Iimura, Y.; Koizumi, H. The Effect of Dense Understory Dwarf Bamboo (*Sasa senanensis*) on Soil Respiration before and after Clearcutting of Cool Temperate Deciduous Broad-leaved Forest. *Ecol. Res.* **2012**, *27*, 577–586.
39. Lefevre, R.; Barre, P.; Moyano, F.E.; Christensen, B.T.; Bardoux, G.; Eglin, T.; Girardin, C.; Houot, S.; Katterer, T.; van Oort, F.; et al. Higher Temperature Sensitivity for Stable than for Labile Soil Organic Carbon–Evidence from Incubations of Long-term Bare Fallow Soils. *Glob. Change Biol.* **2014**, *20*, 633–640. [CrossRef]
40. Aoyama, M. Estimation of Microbial Biomass in Ando Soils by Measurement using a Handy Iuminometer. *Jpn. Soc. Microbiol.* **2005**, *59*, 41–44.
41. Fontaine, S.; Bardoux, G.; Abbadie, L.; Mariotti, A. Carbon Input to Soil may decrease Soil Carbon content. *Ecol. Lett.* **2004**, *7*, 314–320. [CrossRef]
42. Jones, D.L.; Edward, A.C. Influence of Sorption on the Biological Utilization of Two Simple Carbon Substrates. *Soil Biol. Biochem.* **1998**, *30*, 1895–1902. [CrossRef]
43. Kuzyakov, Y. Priming Effects: Interactions between Living and Dead Organic Matter. *Soil Biol. Biochem.* **2010**, *42*, 1363–1371. [CrossRef]
44. Anderson, J.P.E.; Domsch, K.H. A Physiological Method for the Quantitative Measurement of Microbial Biomass in Soils. *Soil Biol. Biochem.* **1978**, *10*, 215–221. [CrossRef]
45. Yuan, Y.; Zhang, Z.; Chen, L.; Yang, C. The Formation of Protected SOM Facilitated by Labile C Input via Artificial Roots. *Eur. J. Soil Sci.* **2020**, *100*, 103231. [CrossRef]
46. Schmidt, M.W.I.; Torn, M.S.; Abiven, S.; Dittmar, T.; Guggenberger, G.; Janssens, I.A.; Kleber, M.; Kogel−Knabner, I.; Lehmann, J.; Manning, D.A.C.; et al. Persistence of Soil Organic Matter as an Ecosystem Property. *Nature* **2011**, *478*, 49–56. [CrossRef]
47. Lehmann, J.; Kleber, M. The Contentious Nature of Soil Organic Matter. *Nature* **2015**, *528*, 60–68. [CrossRef]
48. Chen, R.; Senbayram, M.; Bragodatsky, S.; Myachina, O.; Dittert, K.; Lin, X.; Blagodatskaya, E.; Kuzyakov, Y. Soil C and N Availability Determine the Priming Effect: Microbial N Mining and Stoichiometric Decomposition Theories. *Glob. Change Biol.* **2014**, *20*, 2356–2367. [CrossRef]
49. Tao, X.; Yang, Z.; Feng, J.; Jian, S.; Yang, Y.; Bates, C.T.; Wang, G.; Guo, X.; Ning, D.; Kempher, M.L.; et al. Experimental Warming Accelerates Positive Soil Priming in a Temperate Grassland Ecosystem. *Nat. Commun.* **2024**, *15*, 1178. [CrossRef]
50. Li, X.; Feng, J.; Zhang, Q.; Zhu, B. Warming Inhibits the Priming Effect of Soil Organic Carbon Mineralization: A Meta-Analysis. *Sci. Total Environ.* **2023**, *904*, 166170. [CrossRef]

51. Gershenson, J.; Bader, N.E.; Cheng, W. Effects of Substrate Availability on the Temperature Sensitivity of Soil Organic Matter Decomposition. *Glob. Change Biol.* **2009**, *15*, 176–183. [CrossRef]
52. Zhang, S.; Wang, M.; Xiao, L.; Luo, Z. Reconciling Carbon Quality with Availability Predicts Temperature Sensitivity of Global Soil Carbon Mineralization. *Proc. Natl. Acad. Sci. USA* **2024**, *121*, e231384. [CrossRef]